Published in final edited form as:

Exp Mol Pathol. 2015 June ; 98(3): 328–337. doi:10.1016/j.yexmp.2015.03.011.

RGC-32 is a novel regulator of the T-lymphocyte cell cycle

Cosmin A. Tegla[a,b,1], **Cornelia D. Cudrici**[a,1], **Vinh Nguyen**[c], **Jacob Danoff**[a], **Adam M. Kruszewski**[a], **Dallas Boodhoo**[a], **Armugam P. Mekala**[a], **Sonia I. Vlaicu**[a,f], **Ching Chen**[d], **Violeta Rus**[c], **Tudor C. Badea**[e], and **Horea Rus**[a,b,g,*]

[a]Department of Neurology, University of Maryland, School of Medicine, Baltimore, MD, USA

[b]Research Service, Veterans Administration Maryland Health Care System, Baltimore, MD, USA

[c]Department of Medicine, Division of Rheumatology and Clinical Immunology, University of Maryland, School of Medicine, Baltimore, MD, USA

[d]Department of Pathology, University of Maryland, School of Medicine, Baltimore, MD, USA

[e]Retinal Circuit Development and Genetics Unit, N-NRL, National Eye Institute, Bethesda, MD, USA

[f]Department of Internal Medicine, “Iuliu Hatieganu” University of Medicine and Pharmacy, Cluj-Napoca, Romania

[g]Veterans Administration Multiple Sclerosis Center of Excellence, Baltimore, MD, USA

Abstract

We have previously shown that RGC-32 is involved in cell cycle regulation *in vitro*. To define the *in vivo* role of RGC-32, we generated RGC-32 knockout mice. These mice developed normally and did not spontaneously develop overt tumors. To assess the effect of RGC-32 deficiency on cell cycle activation in T cells, we determined the proliferative rates of $CD4^+$ and $CD8^+$ T cells from the spleens of RGC-$32^{-/-}$ mice, as compared to wild-type (WT, RGC-$32^{+/+}$) control mice. After stimulation with anti-CD3/anti-CD28, $CD4^+$ T cells from RGC-$32^{-/-}$ mice displayed a significant increase in [^{3}H]-thymidine incorporation when compared to WT mice. In addition, both $CD4^+$ and $CD8^+$ T cells from RGC-$32^{-/-}$ mice displayed a significant increase in the proportion of proliferating $Ki67^+$ cells, indicating that in T cells, RGC-32 has an inhibitory effect on cell cycle activation induced by T-cell receptor/CD28 engagement. Furthermore, Akt and FOXO1 phosphorylation induced in stimulated $CD4^+$ T-cells from RGC-$32^{-/-}$ mice were significantly higher, indicating that RGC-32 inhibits cell cycle activation by suppressing FOXO1 activation. We also found that IL-2 mRNA and protein expression were significantly increased in RGC-$32^{-/-}$ $CD4^+$ T cells when compared to RGC-$32^{+/+}$ $CD4^+$ T cells. In addition, the effect of RGC-32 on the cell cycle and IL-2 expression was inhibited by pretreatment of the samples with LY294002, indicating a role for phosphatidylinositol 3-kinase (PI3K). Thus, RGC-32 is involved in

*Corresponding author at: University of Maryland, School of Medicine, Department of Neurology, 655 W Baltimore St, BRB 12-033, Baltimore, MD 21201. hrus@umaryland.edu (H. Rus).

[1]Cosmin A. Tegla and Cornelia D. Cudrici contributed equally to this manuscript.

Supplementary data to this article can be found online at http://dx.doi.org/10.1016/j.yexmp.2015.03.011.

Conflict of interest statement

The authors declare that there are no conflicts of interest.

controlling the cell cycle of T cells *in vivo*, and this effect is mediated by IL-2 in a PI3K-dependent fashion.

Keywords

T-cells; Cell cycle; RGC-32; Knockout mouse; Akt; IL-2

1. Introduction

As part of a screen to identify novel genes that are induced by complement activation, we initially cloned *R*esponse *G*ene to *C*omplement (RGC)-32 from rat oligodendrocytes by differential display (Badea et al., 1998). Human and mouse RGC-32 were subsequently cloned as well. RGC-32 expression has been detected in most tissues examined, and it has been found to be involved in cell cycle activation (Badea et al., 1998, 2002). RGC-32 forms a complex with cyclin B1/CDC2, thereby increasing its kinase activity (Badea et al., 2002). Overexpression in human aortic smooth muscle cells leads to S-phase and G2/M entry of unstimulated cells, and C5b-9 further increases the progression to G2/M (Badea et al., 2002). RGC-32 silencing in human aortic endothelial cells abolishes the DNA synthesis induced by C5b-9 and serum growth factors, indicating a requirement for RGC-32 activity for S-phase entry. RGC-32 siRNA-mediated knockdown also significantly reduces C5b-9-induced CDC2 activation and Akt phosphorylation (Fosbrink et al., 2009). In addition, RGC-32 regulates the release of growth factors from these cells (Fosbrink et al., 2009) and is highly expressed by tumor cells. Taken together, these findings suggest that cell cycle induction by C5b-9 is RGC-32-dependent and that this process occurs in part through the regulation of Akt and growth factor release (Fosbrink et al., 2009). These observations using *in vitro* systems have indicated that RGC-32 may play an essential role in cell cycle proliferation. RGC-32 expression is also regulated by steroid hormones, IL-1β, TGF-β, and VEGF (An et al., 2009; Huang et al., 2009; Park et al., 2008; Vlaicu et al., 2008). An increased expression of RGC-32 has been found in peripheral blood mononuclear cells (PBMCs) and the CD14 cells of patients with hyperimmunoglobulin E (IgE) syndrome (Tanaka et al., 2005). In addition, increased levels of RGC-32 expression are found in the PBMCs and CD4 cells of patients with stable relapsing-remitting multiple sclerosis (MS), and their RGC-32 levels significantly decrease during relapses (Tegla et al., 2013).

Thus far, little is known regarding the role of RGC-32 in cell cycle activation and the differentiation of T cells. To better understand the role of RGC-32 in cell proliferation, not only in cultured cells but also in complex organisms such as mice, we targeted the RGC-32 locus by homologous recombination in embryonic stem (ES) cells and generated a RGC-32 knockout mouse, testing its significance for cell cycle activation and its impact on mouse development. We further analyzed its role in cell cycle activation and the differentiation of T cells. Our data show that RGC-32 is involved in regulating the cell cycle activation by T-cell receptor/CD28 engagement *in vivo*, and this effect is mediated by IL-2 in a PI3K-dependent fashion.

2. Materials and methods

2.1. Construction of the targeting vector

The RGC-32 genomic locus was isolated as a recombinant bacteriophage λ clone from a 129/Sv mouse genomic library using a mouse RGC-32 cDNA probe (Badea et al., 2002). The phage isolates obtained after tertiary screening were then purified using a Lambda Maxi kit from Qiagen (Valencia, CA). The lambda DNA obtained was digested with restriction enzymes (*Not*I, *Eco*RI, and *Sal*I). The enzyme digests were subcloned into pBluescript SK (Stratagene), and the positive fragments from Southern analysis were sequenced at the University of Maryland's Biopolymer Lab. A contig was generated on the basis of sequence identity with the mouse genomic sequence published on the NCBI website. Two of the clones resulting from library screening covered exons 3, 4, and 5 and the intron preceding exon 3, and the other two isolated clones covered the rest of the sequence, including exons 1 and 2. The targeting vector consists of: a) the 5′ homology arm of the targeting vector containing a 4-kb Kpn I to Eco RI fragment, ending about 800 bp upstream of exon 1; b) a Frt-PGKNeo-Frt positive selection cassette; c) the 3′ homology arm, spanning about 3 kb, beginning about 300 bp downstream of exon 2; d) the negative selection MC1-TK cassette, and the pBSKS vector backbone. Thus, after homologous recombination, a region spanning exons 1 and 2 is replaced by the FRT-PGKNeo-FRT cassette (Fig. 1A).

2.2. Electroporation and selection of ES cells

The targeting vector was linearized at the 5′ end of the 5′ homology arm and electroporated into W4 ES cells (SV129/SvEvTac line from Taconic Transgenics, Germantown, NY). Electroporation and colony selection were performed by the Transgenic Facility at the University of Maryland in Baltimore on a fee-for-service basis. After electroporation, the ES cells were plated in 10-cm dishes containing a layer of G418-resistant mouse embryo fibroblast feeder cells. Positive selection for the insertion of the phosphoglycerate kinase promoter (PGK)-neomycin resistance gene (neo^r) cassette and negative selection against random integration (which frequently includes the MC1 promoter-thymidine kinase as part of the vector) were achieved by growing the electroporated ES cells for 8–10 days in cell culture medium containing 250 μg/μl G 418 and 2 μM gancyclovir. After 8–10 days in culture, colonies were picked and split into 96-well trays, and genomic DNA extracted from these cells was restriction-digested and screened by Southern blotting for the targeting event. A 600-bp 3′ probe, lying immediately 3′ to the end of the 3′ targeting arm, identified bands of 8.6 and 3.5 kb that corresponded to the WT and disrupted alleles, respectively.

2.3. Generation of mice carrying the disrupted RGC-32 allele

Positive clones were expanded and sent for injection into blastocysts of the C57BL/6NCr mouse strain and then transferred into pseudopregnant females. Chimeric mice, identifiable by agouti coat color, were mated with C57BL/6 mice. Offspring with agouti coat color were tested for the presence of the targeted locus by PCR. Heterozygotes were interbred, and PCR analysis was used to distinguish between offspring with no, one, or two copies of the mutant gene.

2.4. Screening mice for the targeted gene by PCR

DNA for PCR analysis was prepared from mouse tails using DNA Easy kits (Qiagen). For the targeted allele, a 660-bp product was generated using two sets of primers: 5′-GCTTCCTCGTGCTTTACGGTATCG-3′ and 5′-GTTGGAAGGCCTGGCTGGACTCCC-3′, situated in the neo cassette, and 5′-GCGTCTAGAGGCTCAGGCGAGTAGCTAGCGCTC-3′ and 5′-GGACTGCTCTGCGCTGAGGGCGGC-3′ to check the deletion of exon 1 in RGC-32 to give a product of 176 bp.

2.5. Southern blotting

Southern blot analysis of genomic DNA extracted from ES clones and mouse tails was performed as described. Genomic DNA was extracted using DNA Easy kits (Qiagen). Genomic DNA extracted from the ES clones was digested with *Eco*RV. The DNA samples were electrophoresed in a 0.5% TBE agarose gel and transferred to nitrocellulose paper, followed by crosslinking in a UV Stratalinker (Stratagene, La Jolla, CA). Hybridization with specific cDNA probes was carried out by incubating the nitrocellulose paper with a ^{32}P-labeled RGC-32 probe for 24 h at 37 °C. Nitrocellulose papers were sequentially washed then exposed to BioMax Kodak film at −80 °C.

2.6. Northern blotting

Total RNA was purified from mouse tissues using an RNEasy purification kit (Qiagen). The RNA samples were electrophoresed in a 0.8% agarose-formaldehyde gel, transferred to nitrocellulose paper, and crosslinked with a UV Stratalinker. Hybridization with specific cDNA probes was carried out by incubating the nitrocellulose paper with ^{32}P-labeled cDNA probes for 24 h at 37 °C. After washing, the nitrocellulose papers were then exposed to BioMax Kodak film at −80 °C.

2.7. Western blotting

Western blotting was performed as previously described (Fosbrink et al., 2006). Mouse tissues were minced using scissors and homogenized in liquid nitrogen using a mortar and pestle. Tissues were further lysed in a buffer consisting of 10 mM Tris-HCl (pH 7.4), 1 mM EDTA, 1 mM EGTA, 1 mM NaF, 20 mM $Na_4P_2O_7$, 1% Triton X-100, 0.1% SDS, 100 mM NaCl, 10% glycerol, 0.5% sodium deoxycholate, 1 mM Na_3VO_4, and complete mini protease inhibitor mixture (Roche Applied Science, Indianapolis, IN), which was added just prior to use. Protein concentrations were determined using a BCA protein assay kit (Pierce, Rockford, IL). Samples were fractionated on an SDS-polyacrylamide gel and transferred to a nitrocellulose membrane (Millipore, Bedford, MA). The membrane was blocked with 0.1% Tween-TBS containing 1% bovine serum albumin (BSA) for 1 h and incubated with rabbit IgG anti RGC-32 overnight at 4 °C. Goat anti-rabbit IgG-HRP conjugated antibody (Santa Cruz Biotech, Santa Cruz, CA) was applied for 1 h at room temperature. After washing, the immune complexes were detected using enhanced chemiluminescence (Pierce). Membranes were stripped using Restore Western Blot Stripping Buffer (Pierce) and reprobed for the expression of β-actin (Rockland Immunochemicals, Rockville, MD), and the results were expressed as a ratio to β-actin. Western blotting for pAKT1 and pFOXO1

was performed using rabbit IgG specific for Akt phosphorylated at Ser 473 (CST, Danvers, MA) and FOXO1 phosphorylated at Ser 256 (CST), respectively, and the results were expressed as a ratio to Akt and FOXO1, respectively, as previously described (Fosbrink et al., 2006). The radiographic band density was measured using UN-SCAN-IT software (Silk Scientific, Orem, UT).

2.8. Immunohistochemical localization for RGC-32

Immunohistochemical staining for RGC-32 was performed as previously described (Cudrici et al., 2007). The air-dried cryostat sections (4–6 μm) were fixed for 10 min in acetone containing 0.3% H_2O_2 to remove endogenous peroxidase. Tissue sections and cytospins were blocked for 10 min with 2.5% horse serum, then incubated overnight at 4 °C with rabbit anti-RGC-32 as previously described (Fosbrink et al., 2005). The slides were washed three times for 3 min with PBS, pH 7.4, and then processed using the RTU Vecastain universal kit (Vector Labs, Burlingame, CA) according to the manufacturer's instructions. Specific reactions were developed using NovaRED (Vector Labs) as a substrate; the slides were then counterstained with Harris's hematoxylin (Sigma, St. Louis, MO) and mounted with permanent mount.

2.9. CD4 isolation T-cells isolation

$CD4^+$ T lymphocytes were isolated from mouse spleens using an EasySep Negative Mouse CD4 kit (STEMCELL, Vancouver, Canada) as previously described (Nguyen et al., 2012). In brief, a mouse $CD4^+$ T-cell enrichment cocktail was added at 50 μl/ml of cells, followed by the addition of biotin selection cocktail and then addition of the D2 magnetic particles for 5 min. The magnetically labeled, unwanted cells were separated by using the EasySep magnet, and the enriched cells were used for further processing.

2.10. [^{3}H]thymidine incorporation

DNA synthesis testing was performed as previously described (Fosbrink et al., 2009; Niculescu et al., 1997). CD4 cells isolated as described above were plated on 96-well plates pre-coated with anti-CD3 (5 μg/ml) and anti-CD28 (1 μg/ml) then incubated for 48 h. After stimulation, 1 μCi/ml of [^{3}H]thymidine (Perkin Elmer, Boston MA) was added to the cells. The plate was incubated at 37 °C with 5% CO_2 for 18 h. The cells were lysed and precipitated by adding 20% trichloroacetic acid, and the precipitated DNA was filtered through Whatman GF/A filter paper (Whatman, Maidstone, UK). The filter paper was air-dried, and the radioactivity was counted by liquid scintillation.

2.11. FACS analysis

Intracellular staining using CD4-PE (Biolegend), CD8-PE (Biolegend), and Ki-67 was performed using the FOXP3 Buffer Staining Set (eBioscience) according to the manufacturer's protocol. The anti-Ki-67 FITC was obtained from eBiosciences and used according to the manufacturer's protocol, and the cells were analyzed by flow cytometry within 1 h of staining. Multicolor flow cytometric analyses were performed using a FACScan, Accuri C6, and LSR II flow cytometer (BD Biosciences). Lymphocytes were

gated for forward and side scatter, and fluorescence data were collected for a minimum of 10,000 gated cells.

2.12. Real-time PCR

Real-time PCR was performed using a StepOne real-time PCR system (Applied Biosystems, Foster City, CA). The primers for the genes investigated were designed and synthesized by IDT (Coralville, IA) and used in conjunction with LightCycler FastStart DNA Master SYBR Green I (Roche) as previously described (Tegla et al., 2013). As a negative control for each real-time PCR assay, the same reaction was performed in the absence of cDNA or reverse transcriptase. For each gene, the cycle threshold (C_T) values were determined in the exponential phase of the amplification plot and normalized by subtraction of the C_T value for 18S (generating a ΔC_T value). The results were normalized to the L13 ribosomal protein. In some cases, the fold change in target gene samples, after normalization with the housekeeping gene (18S), was calculated using the $2^{-\Delta\Delta CT}$ value, where $\Delta\Delta C_T = \Delta C_T$ (sample) − ΔC_T (control) and ΔCT is the C_T value of target gene normalized to the C_T value of the housekeeping gene (Cudrici et al., 2008). A real-time PCR array containing genes activated after CD3/CD28 stimulation and implicated in the proliferation of $CD4^+$ T cells (Bio-Rad Labs, Hercules, CA) was processed according to the manufacturer's instructions.

3. Results

3.1. Generation and characterization of RGC-32 KO mice

The mouse *RGC-32* locus is located on chromosome 14 and has 5 exons. We isolated several mouse genomic clones for RGC-32, and generated a targeting construct for RGC-32. Our targeting strategy involved replacing 2-kb of genomic sequence spanning part of the promoter and the first two exons of the RGC-32 gene with a PGK-Neo selection marker (Fig. 1A). This strategy should result in ablating the transcription and translation start sites of the gene, the first two exons, the splice donor junction of exon 2, remove the first 79 amino acids, and result in a frameshift beginning with exon 3. In addition, the PGKNeo expression cassette contains a transcription STOP signal, thus precluding expression of exons 3 to 5 from any upstream alternative transcription start sites. Thus, this strategy will likely result in a complete loss of function RGC-32 allele. The targeting vector contained a 6-kb 5′ homology arm, followed by an Frt-PGKNeo-Frt positive selection cassette, a 3-kb 3′ homology arm, and the negative selection MC1-TK cassette. After electroporation into W4 ES cells (SV129/SvEvTac line and colonies selection) DNA was extracted from these cells, restriction-digested with *Eco*RV and screened by Southern blotting for the targeting event (Fig. 1B). Chimeric mice generated from ES cells were crossed with C57BL/6 females to generate heterozygous, RGC-32 WT/null mice. The F1s were then backcrossed to generate homozygous null, RGC-32 null/null, and littermate controls, RGC-32 WT/null, and RGC-32 WT/WT. To identify the WT and knockout alleles, we used Southern blot analysis of DNA extracted from mouse tails (Fig. 1C). In addition, in order to phenotype the offspring, we used specific primers and conventional PCR (Fig. 1D).

The absence of RGC-32 mRNA expression and protein in the mutant mice was confirmed by Northern blotting (Fig. 2A) and Western blotting (Fig. 2B). As shown in Fig. 2A, no

RGC-32 mRNA expression was found in the tissues obtained from RGC-32$^{-/-}$ mice, but abundant expression was seen in the lungs, thymus, and kidneys of the WT mice. The RGC-32 protein was not detected in RGC-32$^{-/-}$ mice by Western blotting. We did not see the band at about 15 kDa that is typical of the RGC-32 protein (Fig. 2B). In WT mice, the highest expression was again found in the lungs, thymus, and kidneys (Fig. 2B). To further confirm the data obtained by Western blotting and to identify the cells that express RGC-32, we next localized RGC-32 expression by immunohistochemical staining in tissues from WT and RGC-32$^{-/-}$ mice. A significant amount of RGC-32 protein expression was found in the WT mice in the cerebellum, where Purkinje cells showed significant expression (Fig. 3A); we also saw considerable expression in the lung bronchiolar epithelium (Fig. 3C) and the thymus (Fig. 3E). Sectioning of the thymus (Fig. 3E) showed a portion of the darker-colored cortex with closely packed lymphocytes, and a portion of the lighter-colored medulla with more widely spaced lymphocytes. RGC-32 is expressed by clusters of cortical thymocytes. Some medullar T cells showed weak RGC-32 expression (Fig. 3E). In the kidneys, the renal tubular cells displayed intense staining (Fig. 3G), and in the spleen, RGC-32-stained cells were found in the periarteriolar lymphoid sheets and germinal centers (Fig. 3I). There was no expression of RGC-32 in RGC-32$^{-/-}$ mouse tissues (Fig. 3B, D, F, H and J).

Approximately 15% of the offspring born in RGC-32$^{+/-}$ × RGC-32$^{+/-}$ crosses were found to be RGC-32$^{-/-}$ in genotype, indicating some embryonic lethality. At birth, these homozygotes were indistinguishable from their WT and heterozygous littermates. Mice lacking RGC-32 did not display any gross anatomical or histological abnormalities, and they had a normal life expectancy. RGC-32$^{-/-}$ mice did not display any significant phenotypic changes when compared to WT mice. In addition, their growth curves were similar (Supplemental Fig. 1).

3.2. Effect of RGC-32 on cell cycle activation in T cells

CD3/CD28 co-stimulation initiates a series of intracellular signals that increase cellular metabolism, oppose cell death, and drive progression through the cell division cycle (Appleman et al., 2002). Using *in vitro* CD3/CD28 co-stimulation of T cells isolated from spleen we next explored the role of RGC-32 in cell cycle activation. There was a statistically significant increase in [^{3}H]thymidine-induced incorporation into unstimulated RGC-32$^{-/-}$ CD4$^+$ cells *vs.* WT cells ($p < 0.03$) (Fig. 4A). The thymidine uptake caused by stimulation with anti-CD3/CD28 was also significantly higher in RGC-32$^{-/-}$ CD4$^+$ cells than in WT cells ($p < 0.01$) (Fig. 4A). As shown in Fig. 4B, anti-CD3/CD28 co-stimulation induced a significant increase in the CD4$^+$ T-cells from RGC-32$^{-/-}$ mice when compared to CD4$^+$ obtained from WT mice ($p < 0.01$). Similarly, we found that both CD4$^+$ and CD8$^+$ cells displayed a higher percentage of Ki-67-positive CD4 and CD8 cells in RGC-32$^{-/-}$ mice stimulated with anti-CD3/CD28 ($p < 0.0007$ for CD4$^+$ and $p < 0.05$ for CD8$^+$) (Fig. 4C). These data clearly indicate that in T cells, RGC-32 plays an important role in inhibiting cell cycle activation, since the proliferation of these cells was significantly increased in the absence of RGC-32.

CD3/CD28 co-stimulation initiates a series of intracellular signals, and ligation-dependent tyrosine phosphorylation of CD28 enables the recruitment and activation of PI3K, resulting

in the intracellular accumulation of 3-phosphorylated lipids (Pages et al., 1994; Ward et al., 1993). The lipid products of PI3K bind pleckstrin homology domain-containing proteins, including the serine/threonine kinase Akt (Kane et al., 2001). Since the PI3K/Akt pathway plays an important role in cell cycle activation, we examined the effect of LY294002 (a specific PI3K inhibitor) on cell cycle induction by CD3/CD28 co-stimulation. As shown in Fig. 4D, pretreatment with LY294002 significantly reduced ($p < 0.01$) the cell cycle activation induced by CD3/CD28 stimulation.

3.3. Effect of RGC-32 on Akt1 and FOXO1 phosphorylation in T cells

Since Akt1 is a major player in the activation of the cell cycle (Kane et al., 2001; Rathmell et al., 2003) and in cell survival (Datta et al., 1999; Jones et al., 2000), we next investigated the effect of CD3/CD28 co-stimulation on Akt activation in RGC-32$^{-/-}$ CD4^{+} T cells. Akt phosphorylation (Ser 473) was significantly higher in RGC-32$^{-/-}$ CD4^{+} T cells stimulated with anti-CD3/CD28 for 1 h ($p < 0.05$) than in CD4^{+} T cells from WT mice (Fig. 5), suggesting a role for Akt1 in the robust induction of the cell cycle in RGC-32$^{-/-}$ mice. Among the molecular targets of Akt, the mammalian Forkhead box, class O (FOXO) family of Forkhead transcription factors plays a critical role in the regulation of proliferation and apoptosis (Tzivion et al., 2011). Growth factor or antigenic stimulation induces phosphorylation of FOXO proteins by the serine/threonine kinase Akt on three consensus sites, resulting in their nuclear exclusion and sequestration in the cytosol, preventing FOXO1 activation and promoting cell cycle activation (Fosbrink et al., 2006; Salih and Brunet, 2008; Tzivion et al., 2011). Through their function as transcription factors, FOXO proteins regulate the expression of cell cycle regulators such as the cyclin-dependent kinase inhibitor p27 (Machida et al., 2003; Potente et al., 2003; Stahl et al., 2002) and pro-apoptotic genes such as FasL and Bim (Brunet et al., 1999; Stahl et al., 2002). We next examined the phosphorylation of FOXO1 in RGC-32$^{-/-}$ mice, compared to that in WT mice. Significantly higher levels of p-FOXO1 (Ser 256) were found in the RGC-32$^{-/-}$ mice at 30 min and 1 h ($p < 0.01$) of CD3/CD28 stimulation, and FOXO1 phosphorylation declined at 3 h of stimulation (Fig. 6). In contrast, the highest levels of p-FOXO1 were found at 3 h of stimulation in WT mice (Fig. 6), but these levels were not significantly different from those in RGC-32$^{-/-}$ mice. These data suggest that significantly higher levels of cell cycle activation induced by CD3/CD28 stimulation in RGC-32$^{-/-}$ CD4^{+} T-cells are associated with an earlier and robust phosphorylation of FOXO1.

3.4. Genes activated by CD3/CD28 stimulation and implicated in CD4^{+} T-cell proliferation

To gain more insight into other factors that might be involved in cell cycle activation by anti-CD3/CD28 co-stimulation in CD4^{+} T cells from RGC-32$^{-/-}$ mice, we used a real-time PCR array containing 40 genes involved in activation that are implicated in the proliferation of CD4^{+} T cells. We compared the expression profile of these genes in RGC-32$^{-/-}$ CD4^{+} T cells with those from WT mice 6 h after stimulation with anti-CD3/CD28 (Table 1). Genes up-regulated or down-regulated by 2.5-fold or more were considered significantly increased. We found that genes belonging to the PI3K/Akt, NF-kB, Stat5, and MAPK pathways were increased in RGC-32$^{-/-}$ CD4^{+} T cells when compared to those from WT mice (Table 1). We also found that IL-2 mRNA expression was increased in RGC-32$^{-/-}$ mice by 2.5 fold when compared to WT mice (Table 1). This increase was confirmed in separate time-course

experiments with mRNA for IL-2 (Fig. 7A). The increase in IL-2 mRNA in RGC-32$^{-/-}$ CD4^{+} T cells was statistically significant at 24 h of stimulation ($p < 0.05$).

When protein levels of IL-2 were measured by ELISA in the culture supernatants after anti-CD3/CD28 stimulation, we found a similar significant increase in the IL-2 protein secreted by CD4^{+} T-cells (Fig. 7B). In addition, IL-2 expression was inhibited by pretreatment of the samples with LY294002 (Fig. 7B), indicating a role for PI3K in the induction of IL-2 expression. All these data indicate an important role for RGC-32 in mediating CD4 T-cell proliferation through the modulation of IL-2 expression.

4. Discussion

RGC-32 has been implicated in the regulation of the cell cycle and apoptosis (Badea et al., 2002; Fosbrink et al., 2009; Tegla et al., 2013). Although the role of RGC-32 has been extensively examined in smooth muscle, endothelial, and tumor cells in culture, little is known about its role *in vivo*. To better understand the role of RGC-32 in cell proliferation, we targeted the RGC-32 locus by homologous recombination in embryonic stem cells and generated a RGC-32 knockout mouse. In this study, we report that RGC-32 plays an important role in the regulation of the cell cycle *in vivo*. Our experiments indicate that in the absence of RGC-32, an increased proliferation of T cells occurs when compared to WT T cells. The increased proliferation seen in RGC-32$^{-/-}$ CD4^{+} T cells after CD3/CD28 co-stimulation is mediated at least in part by activation of the PI3K pathway (Fig. 8).

Among the several targets of the PI3K pathway, Akt and the transcription factor FOXO1 play an important role in the control of cell cycle progression in the immune system (Salih and Brunet, 2008; Tzivion et al., 2011). Upon stimulation by growth factors or an antigen receptor, the FOXO1 protein becomes phosphorylated on its three consensus sites for Akt, inhibiting its activity as a transcription factor, and thus allowing optimal cell proliferation (Salih and Brunet, 2008; Tzivion et al., 2011). Interestingly, we found that FOXO1 phosphorylation at Ser256 was significantly higher and occurred earlier in RGC-32$^{-/-}$ than in WT CD4^{+} T cells after anti-CD3/CD28 stimulation.

Consistent with FOXO1 phosphorylation, TCR/CD28-induced Akt activation was also stronger in CD4^{+} T cells obtained from RGC-32$^{-/-}$ mice. These data suggest that RGC-32 has an inhibitory effect of the Akt/FOXO1 pathway in CD4^{+} T cells. This finding was in contrast to the effect of RGC-32 in endothelial cells, where RGC-32 was found to physically associate with Akt and to be phosphorylated by Akt *in vitro* after stimulation with C5b-9. Mutation of RGC-32 protein at Ser 45 and Ser 47 prevented the Akt-mediated phosphorylation (Fosbrink et al., 2009). In addition, RGC-32 was found to stimulate the cell cycle in human aortic endothelial cells (Fosbrink et al., 2009), unlike the results in T cells, where RGC-32 had an opposite effect on the cell cycle.

The effects of RGC-32 on T-cell proliferation were similar to those seen in tumor cells (Vlaicu et al., 2010). Since RGC-32 can induce the cell cycle in primary cells (Badea et al., 1998, 2002; Fosbrink et al., 2009), this protein may play a dual role: as an activator of the cell cycle in primary cells, and as a tumor suppressor in cancer cells or an inhibitor of the

cell cycle in some primary cells. Such dual roles have been reported for other proteins involved in cell cycle activation, such as TGF-β (Jakowlew, 2006) and RUNX1 (Wotton et al., 2008), which can either inhibit or stimulate the cell cycle, depending on the cell type and other conditions. It is interesting to note that both RUNX1 (Ito and Miyazono, 2003) and RGC-32 (Tegla et al., 2013) are key targets of TGF-β signaling and that RUNX1 regulates RGC-32 transcription (Tegla et al., 2013).

In both instances, it seems that Akt plays a pivotal role in mediating RGC-32's effects on the cell cycle. It is important to note that the release of growth factors from endothelial cells also plays an important role in the induction of the cell cycle (Fosbrink et al., 2009). In particular, RGC-32 regulates the release of placental growth factor (PlGF) and leptin, which play an important role in cell proliferation, migration, and neovascularization (Fosbrink et al., 2009). Recently, vascular endothelial growth factor receptor 2 (VEGFR2) and PlGF were found to be significantly down-regulated in RGC-32$^{-/-}$ placentas, suggesting that VEGFR2 and PlGF may mediate RGC-32 function in placental angiogenesis (Cui et al., 2013). RGC-32 appears to regulate VEGFR2 expression *via* the activation of NF-kB and to regulate trophoblast proliferation *via* the control of PlGF expression (Cui et al., 2013).

In the case of T cells we found that another growth factor that plays an important role in their proliferation is regulated by RGC-32. We have shown that RGC-32$^{-/-}$ CD4^{+} cells release significantly higher levels of IL-2 after TCR/CD28 stimulation, suggesting an inhibitory role for RGC-32$^{-/-}$ in IL-2 expression and release. IL-2 expression is significantly higher in RGC-32$^{-/-}$ CD4^{+} T cells, and this expression is also dependent on the activation of the PI3K pathway, since LY294002 inhibits IL-2 expression induced by TCR/CD28 stimulation (Fig. 8). IL-2 is a major growth factor in activated T lymphocytes. Upon binding to its receptor, IL-2 activates a variety of signal transduction pathways, including PI3K-mediated proteins that include Akt1, ERK1, and STAT3, all of which are involved in IL-2 mediated cell proliferation (Fung et al., 2003). RGC-32 acts on Akt which phosphorylates FOXO1 protein, induces IL-2 transcription and cell cycle activation contributing to TCR mediated signaling (Fig. 8). Our data also show that RGC-32 exerts many of these effects on the cell cycle by modulating the expression and release of growth factors. Thus, targeting RGC-32 may prove helpful in controlling T-cell proliferation in inflammatory conditions.

Supplementary Material

Refer to Web version on PubMed Central for supplementary material.

Acknowledgments

We thank Dr. Deborah McClellan for editing this manuscript. This work was supported in part by Veterans Administration Merit Awards BX001458 (to H.R.) and IMMB-002-065 (to H.R.). Dr Sonia Vlaicu's work was partially financed by POSDRU grant no. 159/1.5/S/138776 with the title: "Model colaborativ institutional pentru translatarea cercetarii stiintifice biomedicale in practica clinica-TRANSCENT".

Abbreviations

p-Akt1 posphorylated Akt1

ERK1	extracellular signal-regulated kinase 1
FasL	Fas ligand
FOXP3	Forkhead box P3
FOXO1	Forkhead box protein O1
IL-2	interleukin-2
IL-1β	interleukin-1β
KO	knockout
MAPK	mitogen-activated protein kinases
NF-*k*B	nuclear factor kappa-light-chain-enhancer of activated B cells
p-FOXO1	phosphorylated FOXO1
PI3K	phosphatidylinositol 3-kinase
PlGF	placental growth factor
pAkt1	phosphorylated Akt1
RGC-32	response gene to complement-32
RGC-32$^{-/-}$	RGC-32 Knockout
RGC-32$^{+/-}$	RGC-32 heterozygous
RUNX1	Runt-related transcription factor 1
STAT3	signal transducer and activator of transcription 3
STAT5	signal transducer and activator of transcription 5
TCR T	cell receptor
TGF-β	transforming growth factor-beta
VEGF	vascular endothelial growth factor
VEGFR2	vascular endothelial growth factor receptor 2
WT	wild type

References

An X, et al. Response gene to complement 32, a novel hypoxia-regulated angiogenic inhibitor. Circulation. 2009; 120:617–627. [PubMed: 19652095]

Appleman LJ, et al. CD28 costimulation mediates down-regulation of p27kip1 and cell cycle progression by activation of the PI3K/PKB signaling pathway in primary human T cells. J Immunol. 2002; 168:2729–2736. [PubMed: 11884439]

Badea TC, et al. Molecular cloning and characterization of RGC-32, a novel gene induced by complement activation in oligodendrocytes. J Biol Chem. 1998; 273:26977–26981. [PubMed: 9756947]

Badea T, et al. RGC-32 increases p34CDC2 kinase activity and entry of aortic smooth muscle cells into S-phase. J Biol Chem. 2002; 277:502–508. [PubMed: 11687586]

Brunet A, et al. Akt promotes cell survival by phosphorylating and inhibiting a Forkhead transcription factor. Cell. 1999; 96:857–868. [PubMed: 10102273]

Cudrici C, et al. Dendritic cells are abundant in non-lesional gray matter in multiple sclerosis. Exp Mol Pathol. 2007; 83:198–206. [PubMed: 17662270]

Cudrici C, et al. Complement C5 regulates the expression of insulin-like growth factor binding proteins in chronic experimental allergic encephalomyelitis. J Neuroimmunol. 2008; 203:94–103. [PubMed: 18692252]

Cui XB, et al. Response gene to complement 32 deficiency causes impaired placental angiogenesis in mice. Cardiovasc Res. 2013; 99:632–639. [PubMed: 23695833]

Datta SR, et al. Cellular survival: a play in three Akts. Genes Dev. 1999; 13:2905–2927. [PubMed: 10579998]

Fosbrink M, et al. Overexpression of RGC-32 in colon cancer and other tumors. Exp Mol Pathol. 2005; 78:116–122. [PubMed: 15713436]

Fosbrink M, et al. C5b-9-induced endothelial cell proliferation and migration are dependent on Akt inactivation of Forkhead transcription factor FOXO1. J Biol Chem. 2006; 281:19009–19018. [PubMed: 16670089]

Fosbrink M, et al. Response gene to complement 32 is required for C5b-9 induced cell cycle activation in endothelial cells. Exp Mol Pathol. 2009; 86:87–94. [PubMed: 19162005]

Fung MM, et al. IL-2 activation of a PI3K-dependent STAT3 serine phosphorylation pathway in primary human T cells. Cell Signal. 2003; 15:625–636. [PubMed: 12681450]

Huang WY, et al. RGC-32 mediates transforming growth factor-Î[2]-induced epithelial–mesenchymal transition in human renal proximal tubular cells. J Biol Chem. 2009; 284:9426–9432. [PubMed: 19158077]

Ito Y, Miyazono K. RUNX transcription factors as key targets of TGF-[beta] super-family signaling. Curr Opin Genet Dev. 2003; 13:43–47. [PubMed: 12573434]

Jakowlew SB. Transforming growth factor-beta in cancer and metastasis. Cancer Metastasis Rev. 2006; 25:435–457. [PubMed: 16951986]

Jones RG, et al. Protein kinase B regulates T lymphocyte survival, nuclear factor kappaB activation, and Bcl-X(L) levels in vivo. J Exp Med. 2000; 191:1721–1734. [PubMed: 10811865]

Kane LP, et al. Akt provides the CD28 costimulatory signal for up-regulation of IL-2 and IFN-gamma but not TH2 cytokines. Nat Immunol. 2001; 2:37–44. [PubMed: 11135576]

Machida S, et al. Forkhead transcription factor FoxO1 transduces insulin-like growth factor's signal to p27Kip1 in primary skeletal muscle satellite cells. J Cell Physiol. 2003; 196:523–531. [PubMed: 12891709]

Nguyen V, et al. IL-21 promotes lupus-like disease in chronic graft-versus-host disease through both CD4 T cell- and B cell-intrinsic mechanisms. J Immunol. 2012; 189:1081–1093. [PubMed: 22723520]

Niculescu F, et al. Activation of Ras and mitogen-activated protein kinase pathway by terminal complement complexes is G protein dependent. J Immunol. 1997; 158:4405–4412. [PubMed: 9127005]

Pages F, et al. Binding of phosphatidylinositol-3-OH kinase to CD28 is required for T-cell signalling. Nature. 1994; 369:327–329. [PubMed: 8183372]

Park ES, et al. Response gene to complement 32 expression is induced by the luteinizing hormone (LH) surge and regulated by LH-induced mediators in the rodent ovary. Endocrinology. 2008; 149:3025–3036. [PubMed: 18308847]

Potente M, et al. 11,12-Epoxyeicosatrienoic acid-induced inhibition of FOXO factors promotes endothelial proliferation by down-regulating p27Kip1. J Biol Chem. 2003; 278:29619–29625. [PubMed: 12773534]

Rathmell JC, et al. Activated Akt promotes increased resting T cell size, CD28-independent T cell growth, and development of autoimmunity and lymphoma. Eur J Immunol. 2003; 33:2223–2232. [PubMed: 12884297]

Salih DA, Brunet A. FoxO transcription factors in the maintenance of cellular homeostasis during aging. Curr Opin Cell Biol. 2008; 20:126–136. [PubMed: 18394876]

Stahl M, et al. The Forkhead transcription factor FoxO regulates transcription of p27Kip1 and Bim in response to IL-2. J Immunol. 2002; 168:5024–5031. [PubMed: 11994454]

Tanaka T, et al. Distinct gene expression patterns of peripheral blood cells in hyper-IgE syndrome. Clin Exp Immunol. 2005; 140:524–531. [PubMed: 15932515]

Tegla CA, et al. Dual role of response gene to complement-32 in multiple sclerosis. Exp Mol Pathol. 2013; 94:17–28. [PubMed: 23000427]

Tzivion G, et al. FoxO transcription factors; regulation by AKT and 14-3-3 proteins. Biochim Biophys Acta. 2011; 1813:1938–1945. [PubMed: 21708191]

Vlaicu SI, et al. Role of response gene to complement 32 in diseases. Arch Immunol Ther Exp (Warsz). 2008; 56:115–122. [PubMed: 18373239]

Vlaicu SI, et al. Epigenetic modifications induced by RGC-32 in colon cancer. Exp Mol Pathol. 2010; 88:67–76. [PubMed: 19883641]

Ward SG, et al. Ligation of CD28 receptor by B7 induces formation of D-3 phosphoinositides in T lymphocytes independently of T cell receptor/CD3 activation. Eur J Immunol. 1993; 23:2572–2577. [PubMed: 8405057]

Wotton S, et al. Gene array analysis reveals a common Runx transcriptional programme controlling cell adhesion and survival. Oncogene. 2008; 27:5856–5866. [PubMed: 18560354]

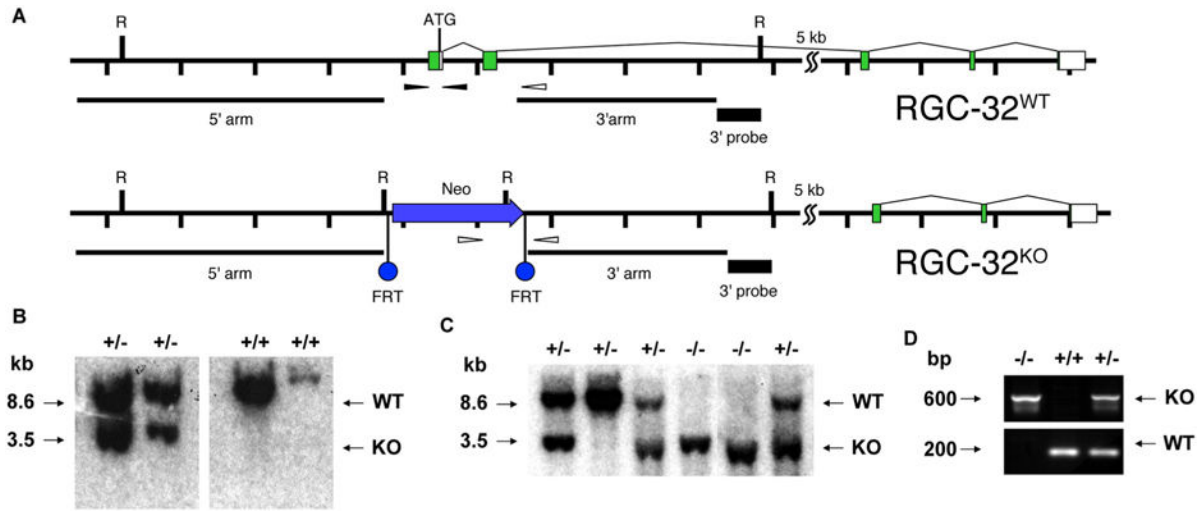

Fig. 1.

Gene targeting strategy and analysis of genomic DNA. A. Gene-targeting strategy used to generate the null alleles at the RGC-32 locus. Diagrams representing the wild type (top) and targeted (bottom) RGC-32 alleles. Tick marks represent 1 kb distances, except for contracted longer stretches marked with SS marks. Green and white boxes represent coding regions and UTRs respectively, and splice junctions are indicated by angled black lines. Homologous recombination targeting arms (5′ – 4.2 kb and 3′ – 2.7 kb) are indicated by black lines, and the 3′ southern blot probe as a black box under the locus. FRT sites (blue circles) flank the PGK-Neo Cassette. Genotyping primers for the wild type (thin black arrowheads − 167 bp) are spanning exon 1 and encompass the ATG. Genotyping primers for the KO (thin white arrow heads − 600 bp) are placed in the PGK-Neo cassette and the 3′ arm respectively. Eco RV (R) digestion of genomic DNA and hybridization with the indicated 3′ probe result in 8.5 kb (wild type) and 3.5 kb (knock-out) fragments. In the KO allele, exons 1 and 2, including the ATG are removed. B. Southern blot analysis of genomic DNA. Southern blot analysis of genomic DNA extracted from ES clones. The DNA was digested with *Eco*RV and hybridized with probe. The sizes of the wild type (WT) and disrupted (KO) alleles are shown. The genotype of the clones is shown above each lane. C. Southern blot analysis of genomic DNA extracted from mouse tails using a DNA Easy tissue kit (Qiagen). The sizes of the WT and KO alleles are shown. The genotypes of the animals are presented above the lanes. D. PCR amplification of DNA extracted from mouse tails. The sizes of the PCR fragments used to identify the WT and KO alleles are shown. (For interpretation of the references to color in this figure legend, the reader is referred to the web version of this article.)

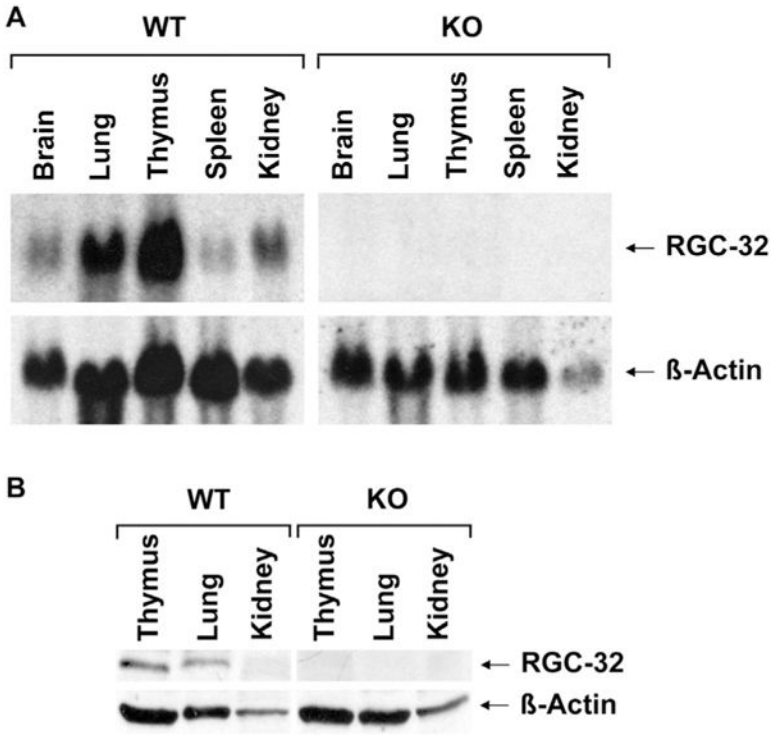

Fig. 2.

RGC-32 expression in mouse tissues. A. RGC-32 mRNA expression analyzed by Northern blotting. Tissue expression of RGC-32 was analyzed by Northern blotting in WT and RGC-32 KO mice. RGC-32 mRNA expression was detected in tissues obtained from the WT mice but not detected in the RGC-32 KO mice. β-Actin was used as a housekeeping gene. B. RGC-32 protein expression analyzed by Western blotting. Tissue expression of RGC-32 protein was analyzed by Western blotting. RGC-32 protein expression was detected in tissue obtained from the WT mice. No RGC-32 protein expression was detected in the RGC-32 KO mice.

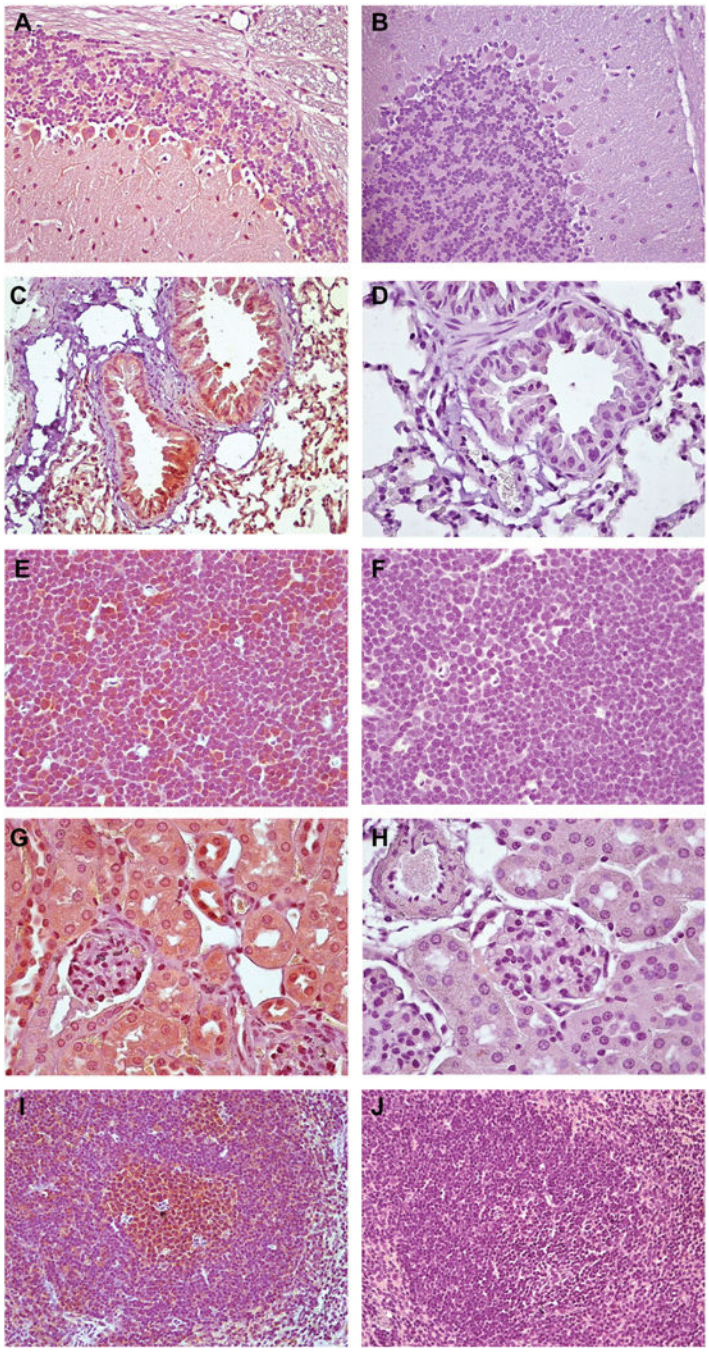

Fig. 3.

Immunohistochemical localization of RGC-32. RGC-32 expression was localized by immunohistochemical staining in tissues from WT and RGC-32$^{-/-}$ mice using a rabbit IgG anti-RGC-32 antibody and a RTU Vectastain universal kit (Vector). A significant amount of RGC-32 protein expression was found in WT mice in Purkinje cells (A), lung bronchiolar epithelium (C), thymus (E), renal tubular cells (G), and spleen, where the stained cells were in the periarteriolar lymphoid sheets and germinal center follicular cells (I). RGC-32

expression was absent from the tissues obtained from the RGC-32$^{-/-}$ mice (B, D, F, H, and J). Original magnification: ×400.

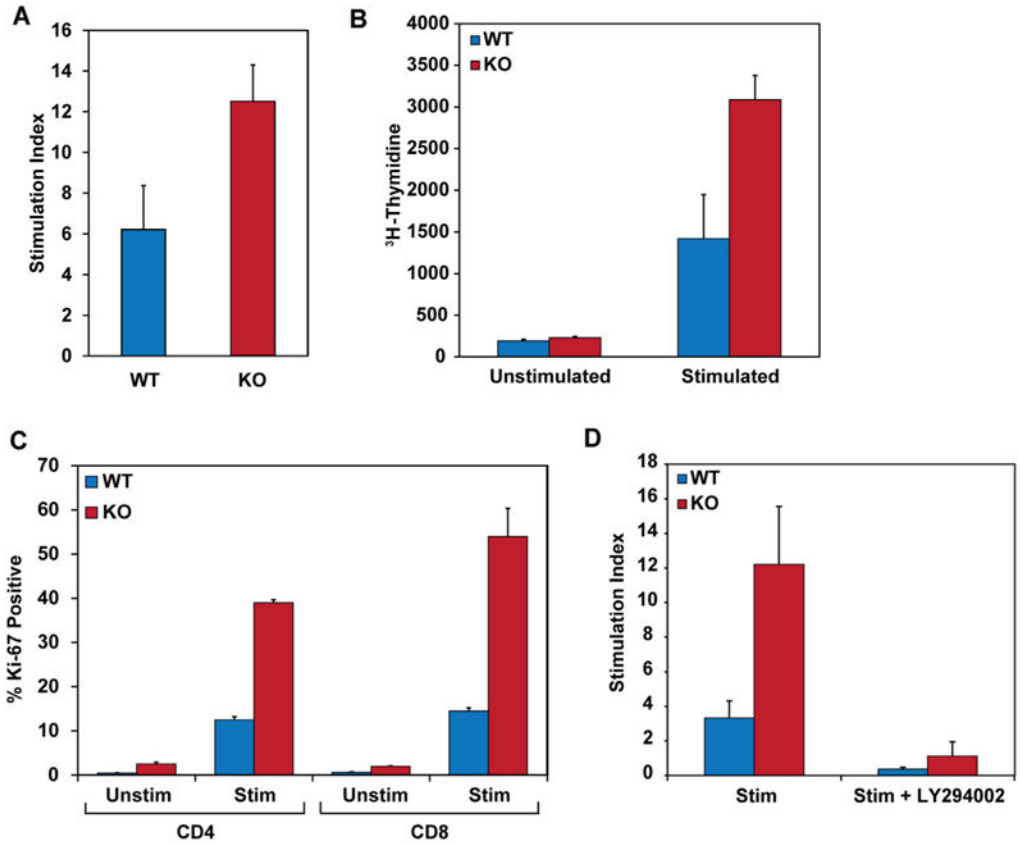

Fig. 4.

RGC-32 suppresses cell proliferation in T cells. A. Splenocytes from WT or KO (RGC-32$^{-/-}$) mice were stimulated with the indicated concentrations of plate-coated anti-CD3 (5 μg/ml) plus soluble anti-CD28 (2.5 μg/ml) mAb for 48 h. [^{3}H]thymidine was added for the final 18 h of culture, and proliferation was measured. Significantly higher levels of [^{3}H]thymidine incorporation were found in RGC-32$^{-/-}$ mice when compared to WT mice. Results (mean ± SEM from three separate experiments) are shown as stimulation index ($p < 0.03$). B. Purified CD4$^+$ T cells from WT or RGC-32$^{-/-}$ mice were stimulated with anti-CD3 (5 μg/ml) plus soluble anti-CD28 (2.5 μg/ml) for 48 h. [^{3}H]thymidine was added for the final 18 h of culture, and proliferation was measured by tritium uptake. Significantly higher levels of [^{3}H]thymidine incorporation were found in CD4$^+$ T cells isolated from spleens of RGC-32$^{-/-}$ mice when compared to WT mice ($p < 0.01$). C. Ki-67 uptake after stimulation with anti-CD3 (5 μg/ml) plus soluble anti-CD28 (2.5 μg/ml) for 48 h was measured in CD4 and CD8 cells isolated from RGC-32$^{-/-}$ and WT mice by FACS analysis. A significant increase in the percentage of Ki-67-positive CD4 ($p < 0.007$) and CD8 ($p < 0.05$) cells was found after stimulation with CD3/CD28 in RGC-32$^{-/-}$ mice when compared to WT mice. D. Effect of LY294002 on cell proliferation. Purified CD4$^+$ T cells from WT or RGC-32$^{-/-}$ mice were stimulated with anti-CD3 (5 μg/ml) plus soluble anti-CD28 (2.5 μg/ml) for 48 h in the presence or absence of LY294002 (10 μM). [^{3}H]thymidine was added for the final 18 h of culture, and proliferation was measured. LY294002 pretreatment significantly reduced the increase in cell proliferation induced after anti-CD3/CD28 stimulation in both WT and RGC-32$^{-/-}$ mice. Results of three separate experiments are expressed as mean ± SEM.

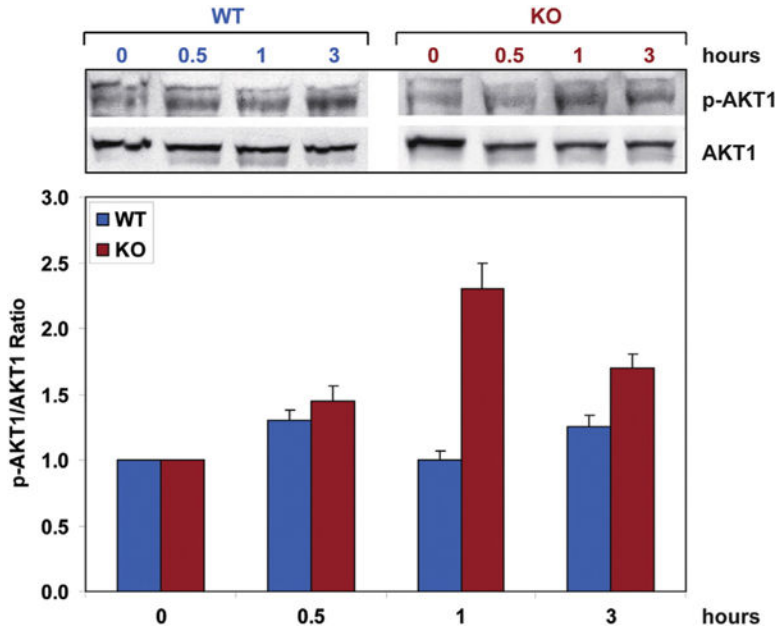

Fig. 5.

RGC-32 regulates Akt phosphorylation in $CD4^+$ T cells. Purified $CD4^+$ T cells from WT or RGC-$32^{-/-}$ mice were stimulated with anti-CD3 (5 μg/ml) and soluble anti-CD28 (2.5 μg/ml) for the indicated periods of time. Cells were lysed, and Akt phosphorylation was assessed by Western blotting with an anti-Akt IgG specific for Akt phosphorylated at Ser 473. The absence of RGC-32 from $CD4^+$ T cells resulted in a significant increase in Akt phosphorylation 1 h after the initiation of co-stimulation ($p < 0.05$). Results of three separate experiments are expressed as mean ± SEM.

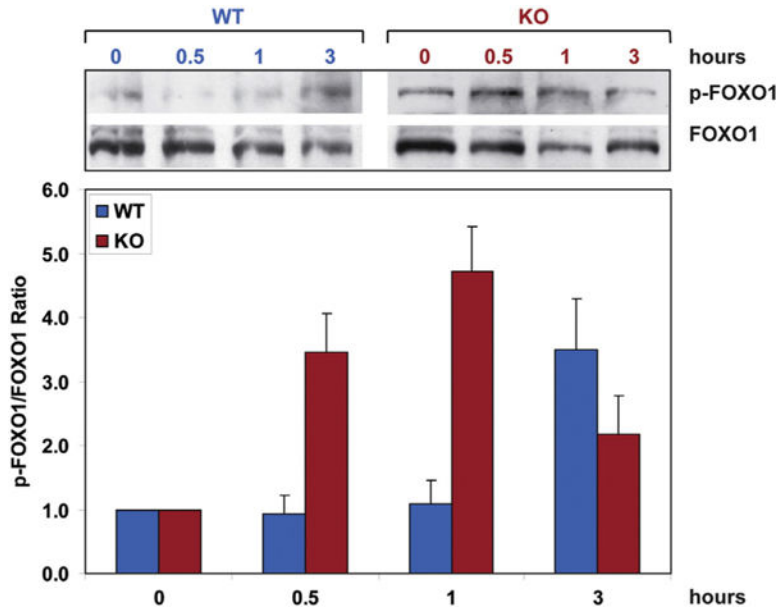

Fig. 6.

RGC-32 regulates FOXO1 phosphorylation in CD4 T cells. Purified $CD4^+$ T cells from WT or RGC-$32^{-/-}$ mice were stimulated with anti-CD3 (5 μg/ml) and soluble anti-CD28 (2.5 μg/ml) for the indicated periods of time. Cells were lysed with RIPA buffer, and FOXO1 phosphorylation was assessed by Western blotting with antibodies specific for FOXO1 phosphorylated at Ser 256 and anti-FOXO1 IgG. In the absence of RGC-32 in $CD4^+$ T cells, a significant increase in FOXO1 phosphorylation was seen at 30 min and 1 h after initiation of co-stimulation ($p < 0.01$) when compared to unstimulated cells. Results of three separate experiments are expressed as mean ± SEM.

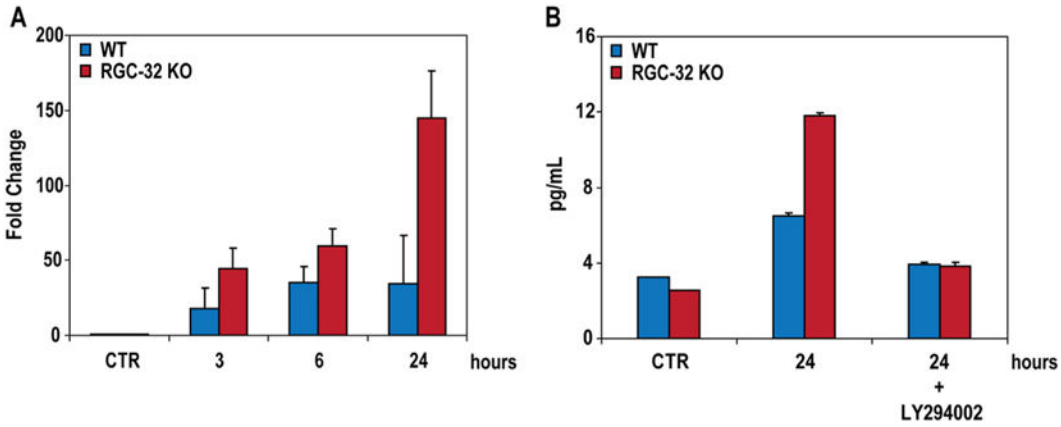

Fig. 7.

RGC-32 regulates IL-2 expression and release. Purified $CD4^+$ T cells from WT or $RGC\text{-}32^{-/-}$ mice were stimulated with anti-CD3 (5 μg/ml) and soluble anti-CD28 (2.5 μg/ml) for the indicated periods of time. A. IL-2 mRNA expression was significantly increased after 24 h of stimulation ($p < 0.05$). B. A similar effect was seen in the IL-2 levels released into the culture supernatant after stimulation. IL-2 protein levels were determined by ELISA. Results of three separate experiments are expressed as mean ± SEM.

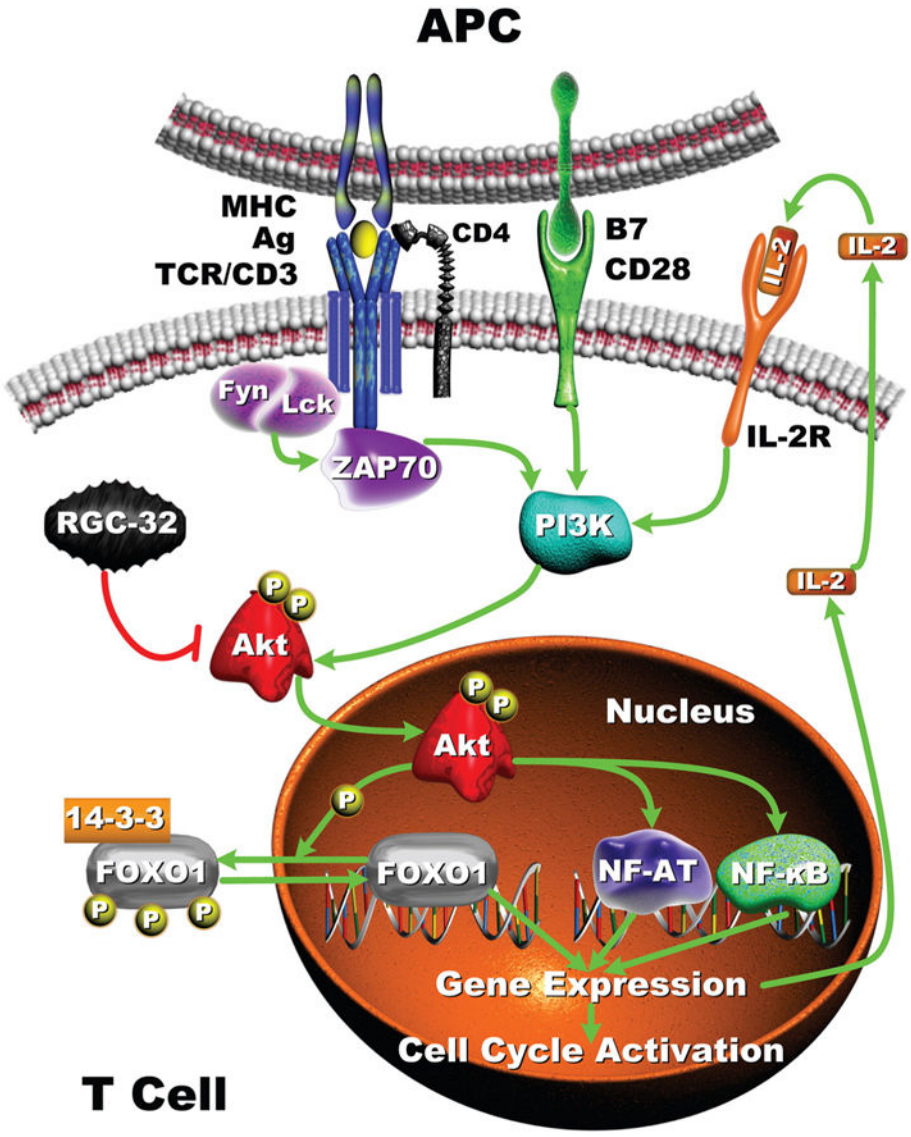

Fig. 8.

Role of RGC-32 in T-cell receptor signaling. Signaling through the T-cell receptor (TCR) is known to involve phosphoinositide 3-kinase (PI3K). The co-stimulatory receptors CD28 contain a consensus PI3K-binding motifs (YXXM), which might also contribute to TCR-dependent PI3K signaling. AKT connects PI3K to signaling pathways that promote cytokine transcription, survival, and cell-cycle activation. RGC-32 acts on Akt which phosphorylates FOXO1 protein, induces IL-2 transcription and cell cycle activation contributing to TCR mediated signaling. Secreted IL-2 has an autocrine effect on T-cells and might be implicated in further activation of PI3K.

Table 1

Genes differentially expressed in RGC-32 KO vs WT mouse $CD4^+$ T cells after stimulation with anti-CD3/CD28 for 6 h.

Gene name	GenBank accession	Fold change
Protein tyrosine phosphatase, non-receptor type 6	NM_013545	13.8
Syk	U25685	9.0
Fos b	NM_008036	7.2
PI3K, regulatory subunit 1 (alpha)	NM_001024955	6.2
Akt2	NM_001110208	6.1
H-ras1	AY373386	5.3
Protein tyrosine phosphatase, non-receptor type 11	NM_011202	5.3
c-Jun	NM_010591	4.4
Akt1	NM_009652	3.8
NF-kB inhibitor alpha	NM_010907	3.7
STAT5a	Z48538	3.5
Rel	NM_009044	3.3
Grb2	NM_008163	3.1
Myc	NM_010849	3.0
Socs3	NM_007707	2.9
Jak1	NM_146145	2.9
STAT5b	Z48539	2.8
Mitogen-activated protein kinase kinase 1	NM_008927	2.7
Interleukin-2	NM_008366	2.7
Mitogen-activated protein kinase 3	NM_011952	2.7
PI3-kinase catalytic subunit beta	NM_029094	2.6
c-Fos	NM_010234	2.6
NF-kB-p50	NM_008689	2.5
IkB kinase beta	NM_010546	2.5